Published in IET Radar, Sonar and Navigation
Received on 21st January 2013
Revised on 28th April 2013
Accepted on 4th June 2013
doi: 10.1049/iet-rsn.2013.0027

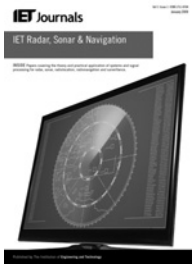

ISSN 1751-8784

Failure correction in time-modulated linear arrays

Lorenzo Poli, Paolo Rocca, Giacomo Oliveri, Andrea Massa

ELEDIA Research Center, Department of Information Engineering and Computer Science, University of Trento, Via Sommarive 5, 38123 Trento, Italy
E-mail: andrea.massa@ing.unitn.it

Abstract: A technique for failure correction in time-modulated linear arrays is presented. Starting from the knowledge of the array elements with failures, the on–off behaviour of the switches at the other elements is properly reconfigured to radiate a pattern as close as possible to the ideal one in terms of pattern features. The array reconfiguration is carried out by solving an optimisation problem through the minimisation of a suitable cost function proportional to the mismatch between ideal and reconfigured pattern features. Representative results are reported and discussed to illustrate the effectiveness of the proposed approach as well as to assess the robustness to failures of time-modulated arrays thanks to their real-time reconfigurability.

1 Introduction

Time-modulated arrays (TMAs) are antenna systems that exploit the time-domain degrees-of-freedom to generate desired radiation patterns. Firstly proposed in [1] and successively analysed in [2, 3] almost half-century ago, TMAs have only recently gained interest from the research community as confirmed by several publications in the past decade where the optimisation of the time-domain parameters, while fitting desired constraints on the radiation performances, has been effectively and efficiently addressed with evolutionary algorithms [4–8]. The technological advances in the design of high-speed radiofrequency (RF) switches [9], used to periodically modulate the static excitations, have further stimulated the proposal of innovative antenna systems based on TMAs. For example, the design of shaped beams has been dealt with in [10], whereas techniques for synthesising the sum and the difference patterns have been proposed in [11–13]. Moreover, non-regular array structures [14, 15] and reflector arrays [16] have been considered also in the presence of real radiating elements [17, 18].

When dealing with TMAs, a key advantage lies in the capability of easily reconfiguring the radiation pattern thanks to the agility in the control of the on–off status of the RF switches. Accordingly, antenna systems based on TMAs have been exploited for adaptive beam-forming [19], interference suppression through pattern nulling [20, 21] and beam steering [22, 23]. Still based on the reconfigurability property of TMAs, an innovative technique for failure correction in time-modulated linear arrays (TMLA) is presented hereinafter. Once the failed elements of the array have been identified by means of a reliable diagnostic technique (e.g. [24, 25]), the pulse sequence controlling the remaining ones is properly re-adapted to yield a pattern close as much as possible to the ideal/nominal one. Towards this end, the problem at hand is recast as an optimisation one devoted to minimise a suitable cost function proportional to the mismatch between the key features [namely the sidelobe level (SLL), half power beamwidth (HPBW) and peak directivity (D)] of the nominal pattern and those of the reconfigured one by means of a particle swarm optimisation (PSO)-based algorithm.

The outline of the paper is as follows. The failure correction problem is mathematically formulated in Section 2 and a set of representative results is then reported and discussed (Section 3) to provide a numerical assessment of the proposed architectural solution. In Section 4, some conclusions are drawn.

2 Mathematical formulation

Let us consider an array of N elements linearly arranged on the Cartesian z-axis with uniform inter-element spacing d. A set of RF switches in the feeding network is used to periodically turn on and off the array elements as shown in Fig. 1. After the low-pass filtering (Fig. 1), the array factor radiated at the carrier frequency $f_0 = (c/\lambda)$, c and λ being the speed of light and the wavelength in free-space, is [2]

$$\mathrm{AF}^{\mathrm{nom}}(\theta) = \sum_{n=1}^{N} \tau_n^{\mathrm{nom}} \mathrm{e}^{\mathrm{j}\left[k(n-1)d\cos\theta+\varphi_n\right]} \tag{1}$$

where φ_n, $n = 1, \ldots, N$ are the weighting coefficients of the phase shifters useful for beam steering (Fig. 1), $k = (2\pi/\lambda)$ is the wavenumber and θ is the angular direction measured from the array axis. Moreover, $\boldsymbol{\tau}^{\mathrm{nom}} = \left\{\tau_n^{\mathrm{nom}}; n = 1, \ldots, N\right\}$ is the reference/nominal pulse duration vector, whose nth entry is given by

$$\tau_n^{\mathrm{nom}} = \frac{1}{T_{\mathrm{p}}} \int_0^{T_{\mathrm{p}}} p_n^{\mathrm{nom}}(t)\, \mathrm{d}t \tag{2}$$

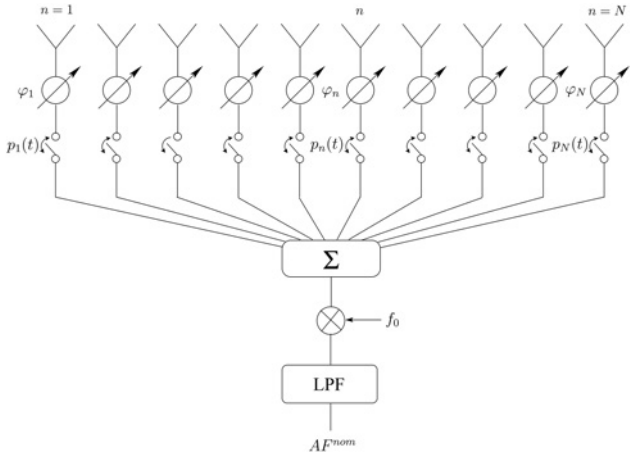

Fig. 1 *Sketch of the time-modulated antenna structure*

where $p_n^{\text{nom}}(t)$ $(n = 1, \ldots, N)$ is the function modelling the periodic pulse of period T_p that controls the on–off of the RF switch at the nth array element. More specifically

$$p_n^{\text{nom}}(t) = \begin{cases} 1, & 0.0 \le t < \tau_n^{\text{nom}} T_\text{p} \\ 0, & \text{otherwise} \end{cases}, \quad n = 1, \ \ldots, \ N \qquad (3)$$

$\tau_n^{\text{nom}} T_\text{p} \left(\tau_n^{\text{nom}} \in [0; 1]\right)$ being the time instant when the nth element is disconnected from the feeding network, whereas all elements are periodically activated at the beginning of the modulation period. Accordingly, the amplitude coefficients of $\text{AF}^{\text{nom}}(\theta)$ defined in (2) are the time averages of the pulse functions in (3) [2].

When the mth, $m \in [1; N]$, element of the array is failed, it follows that $\tau_m^{\text{nom}} \rightarrow \tau_m^{\text{fld}} = 0$ and the array factor radiated by the antenna with failures turns out being modified as follows

$$\text{AF}^{\text{fld}}(\theta) = \text{AF}^{\text{nom}}(\theta) - \sum_{m \in \Upsilon} \tau_m^{\text{nom}} \text{e}^{\text{j}\left[k(m-1)d\cos\theta + \varphi_m\right]} \qquad (4)$$

where Υ being the set of failed elements.

Since $\text{AF}^{\text{fld}}(\theta) \neq \text{AF}^{\text{nom}}(\theta)$, $\theta \in [0; \pi]$, and the differences can be non-negligible, the correction strategy is aimed at keeping a correct functioning of the radiating system by re-configuring the undamaged control points of the TMLA through new pulse sequences, $p_n^{\text{rec}}(t)$, $n \notin \Upsilon$, providing a pattern at f_0

$$\text{AF}^{\text{rec}}(\theta) = \sum_{n=1,\ n \notin \Upsilon}^{N} \tau_n^{\text{rec}} \text{e}^{\text{j}\left[k(n-1)d\cos\theta + \varphi_n\right]} \qquad (5)$$

close as much as possible to $\text{AF}^{\text{nom}}(\theta)$. In (5), τ_n^{rec}, $n = 1,\ldots,$ N, $n \notin \Upsilon$, have the same expression as in (2), but substituting the undamaged functions, $p_n^{\text{nom}}(t)$, $n \notin \Upsilon$, with the pulse sequences, $p_n^{\text{rec}}(t)$, $n \notin \Upsilon$. In order to determine the reconfiguration vector $\boldsymbol{\tau}^{\text{rec}}$, the following cost function

$$\Psi\left(\boldsymbol{\tau}^{\text{rec}}\right) = \sum_{\zeta = \{\text{SLL, HPBW, } D\}} w_\zeta \left\{ \frac{\left|\zeta\left(\boldsymbol{\tau}^{\text{rec}}\right) - \zeta^{\text{nom}}\right|^2}{\left|\zeta^{\text{nom}}\right|^2} \right\} \qquad (6)$$

is minimised. In (6), ζ^{nom} $[\zeta\,(\boldsymbol{\tau}^{\text{rec}})]$ indicates the value of SLL $(\zeta \Leftarrow \text{SLL})$, HPBW $(\zeta \Leftarrow \text{HPBW})$ and the peak directivity $(\zeta \Leftarrow D)$ computed as in [26] of the ideal (i.e. without failures) pattern (1) [the reconfigured one (5)]. Moreover, w_ζ is a real and positive coefficient weighting the ζth term of (6) according to the problem requirements.

Since the unknown vector $\boldsymbol{\tau}^{\text{rec}}$ contains real-valued entries, the optimisation is carried out with PSO according to the guidelines reported in [27]. To improve the convergence, suitably exploiting the available a priori information, a particle of the swarm is set to the value $\boldsymbol{\tau}^{\text{nom}}$, whereas the other particles are randomly generated within the solution space whose bounds are $\tau_{n,\,\text{max}}^{\text{rec}} = 1.0$ and $\tau_{n,\,\text{min}}^{\text{rec}} = 0.0, \forall n \notin \Upsilon$.

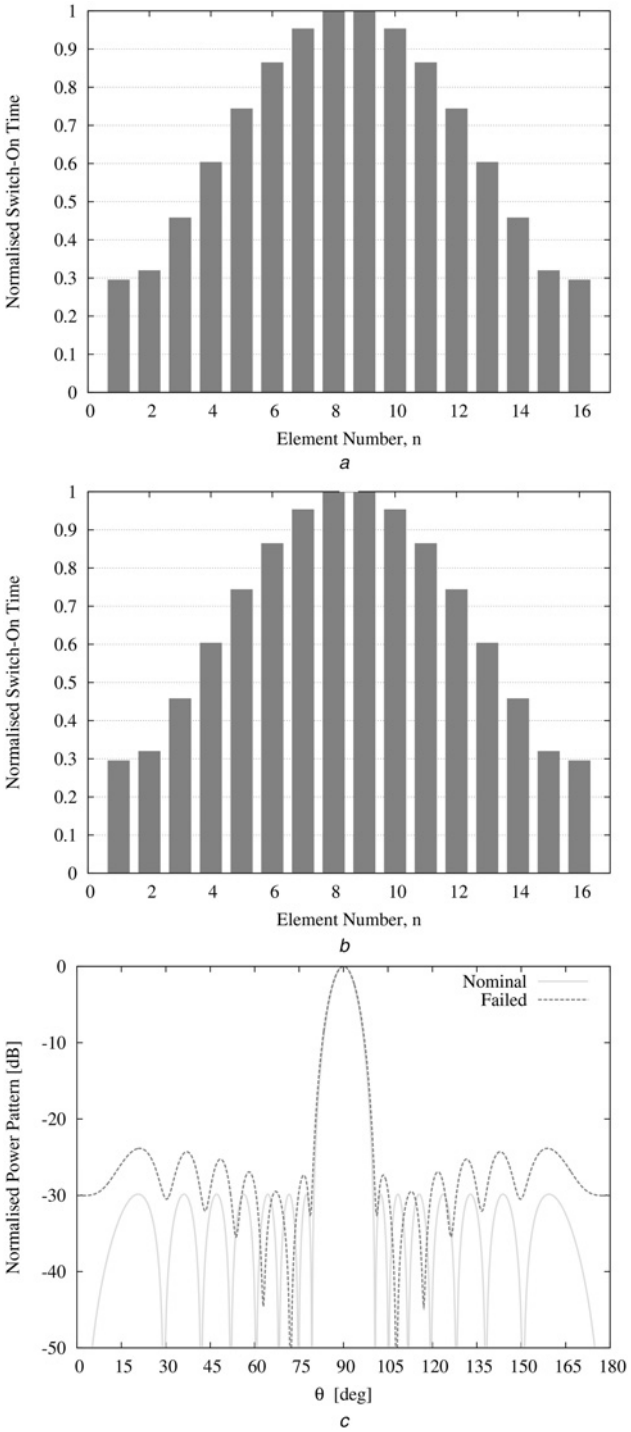

Fig. 2 *Cases A, B and C – [N = 16, d = (λ/2), Dolph–Chebyshev, SLL = − 30 dB, Υ = {2}] – plots of*

a Nominal pulse sequence $\boldsymbol{\tau}^{\text{nom}}$
b Pulse sequence with failure $\boldsymbol{\tau}^{\text{fld}}$
c Corresponding power patterns generated at f_0

doi: 10.1049/iet-rsn.2013.0027

3 Numerical assessment

The examples in the following are devoted to show the behaviour of the proposed approach and the robustness against array element failures of TMLA-based architectures.

In the first example, a linear array with $N = 16$ elements and $d = 0.5\lambda$ is taken into account. With reference to the pulse configuration in Fig. 2*a* affording a nominal Dolph–Chebyshev sum pattern [28] with $\mathrm{SLL}^{\mathrm{nom}} = -30$ dB (Fig. 2*c*) at f_0, let us consider a single failure on the element $m = 2$ (i.e. $\Upsilon = \{2\}$) (Fig. 2*b*). In Fig. 2*c*, the power patterns of both the ideal, $\mathrm{AF}^{\mathrm{nom}}(\theta)$ and that with the failure, $\mathrm{AF}^{\mathrm{fld}}(\theta)$, are given. As it can be observed, although the failed element is in the array tail and the corresponding τ_m^{nom} value is relatively small when compared with other elements (Fig. 2*b*), the whole pattern as well as its key features turn out being seriously compromised (Table 1). Indeed, the SLL increases of > 6 dB ($\mathrm{SLL}^{\mathrm{nom}} = -30.00$ dB against $\mathrm{SLL}^{\mathrm{fld}} = -23.85$ dB) and the beamwidth widens from $\mathrm{HPBW}^{\mathrm{nom}} = 7.96°$ up to $\mathrm{HPBW}^{\mathrm{fld}} = 8.25°$. Only the directivity remains almost unaltered ($\mathrm{D}^{\mathrm{nom}} = 10.20$ dB against $D^{\mathrm{fld}} = 10.06$ dB).

Let us firstly suppose that it is of primary interest (Case A) to reconfigure the antenna to yield a level of the secondary lobes as close as possible to $\mathrm{SLL}^{\mathrm{nom}}$. Towards this purpose, the weights $w_{\mathrm{SLL}} = 1$ and $w_{\mathrm{HPBW}} = w_D = 0$ have been chosen and the PSO has been run with a swarm of $S = N = 16$ particles, inertial weight and cognitive and social acceleration coefficients being set as in [8]. Concerning the stopping criteria of the iterative optimisation, the maximum number of iterations has been set to $I_{\max} = 10^3$ and the convergence threshold for the cost function has been chosen

Table 1 Cases A, B and C – [$N = 16$, , $d = (\lambda/2)$, Dolph–Chebyshev, SLL = −30 dB, $\Upsilon = \{2\}$] – values of the pattern features SLL, HPBW and D and of the SBL and the percentage of SR losses with respect to the total radiated power for the nominal, failed and reconfigured solution when $w_{\mathrm{SLL}} = 1$ and $w_{\mathrm{HPBW}} = w_D = 0$ (Case A), $w_{\mathrm{SLL}} = w_{\mathrm{HPBW}} = w_D = 1$ (Case B) and $w_{\mathrm{SLL}} = 10$ and $w_{\mathrm{HPBW}} = w_D = 1$ (Case C)

	SLL, dB	HPBW, degrees	D, dB	SBL, dB	SR, %
nominal	−30.00	7.96	10.20	−12.39	24.17
failed	−23.85	8.25	10.06	−12.84	22.79
reconfigured: Case A	−29.96	9.16	9.73	−13.79	21.20
reconfigured: Case B	−25.78	8.08	10.19	−12.71	22.21
reconfigured: Case C	−28.48	8.64	9.90	−13.08	22.64

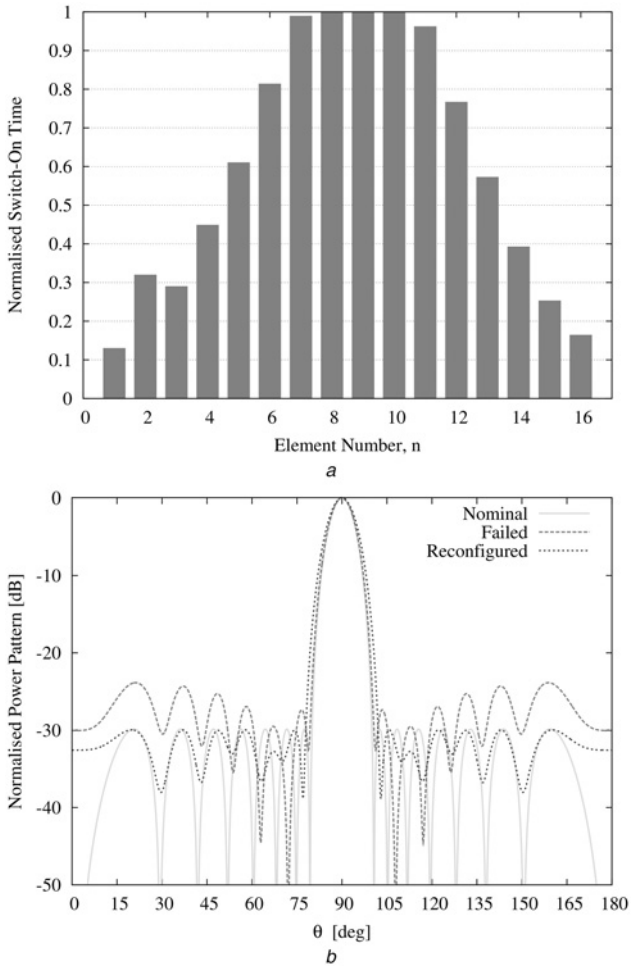

Fig. 3 *Case A – [N = 16, d = (λ/2), Dolph–Chebyshev, SLL = −30 dB, Υ = {2}] – plots of*

a Reconfigured pulse sequence $\boldsymbol{\tau}^{\mathrm{rec}}$

b Corresponding power pattern generated at f_0 together with the nominal and the failed ones when $w_{\mathrm{SLL}} = 1$ and $w_{\mathrm{HPBW}} = w_D = 0$

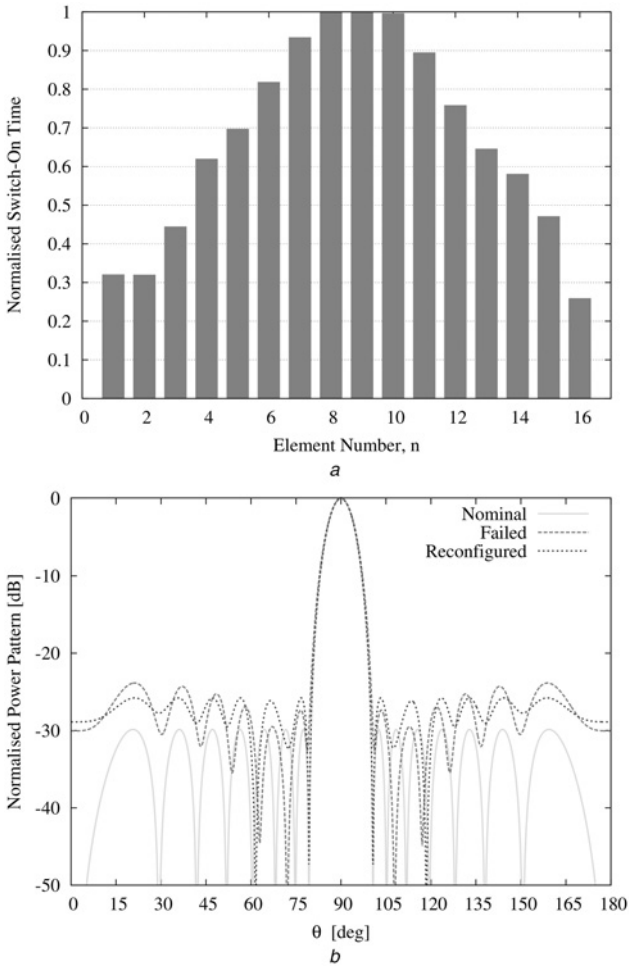

Fig. 4 *Case B – [N = 16, d = (λ/2), Dolph–Chebyshev, SLL = −30 dB, Υ = {2}] – plots of*

a Reconfigured pulse sequence $\boldsymbol{\tau}^{\mathrm{rec}}$

b Corresponding power pattern generated at f_0 together with the nominal and the failed ones when $w_{\mathrm{SLL}} = w_{\mathrm{HPBW}} = w_D = 1$

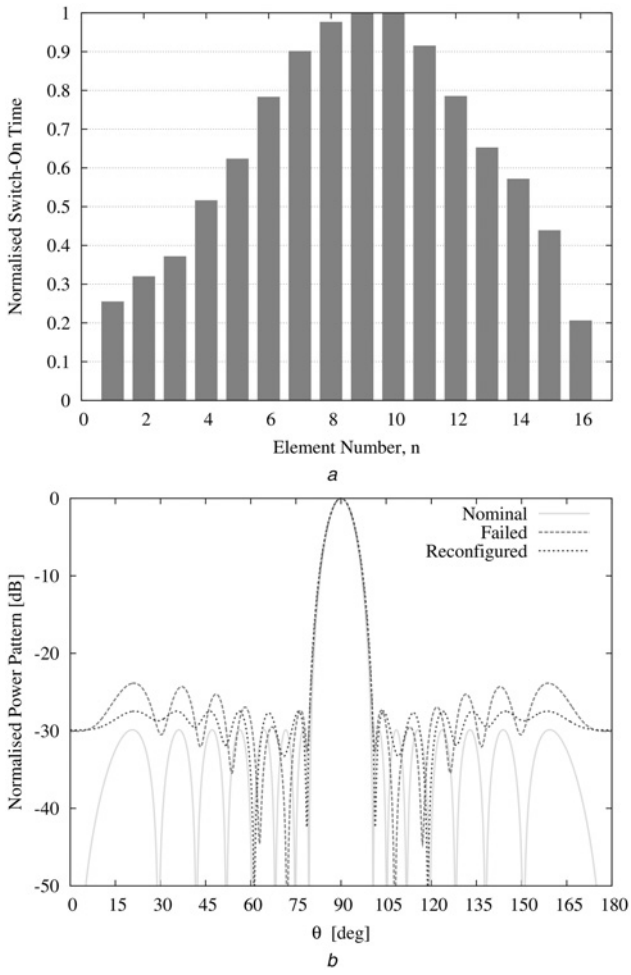

Fig. 5 *Case C – [N = 16, d = (λ/2), Dolph–Chebyshev, SLL = – 30 dB, ϒ = {2}] – plots of*

a Reconfigured pulse sequence $\boldsymbol{\tau}^{\text{rec}}$

b Corresponding power pattern generated at f_0 together with the nominal and the failed ones when $w_{\text{SLL}} = 10$ and $w_{\text{HPBW}} = w_D = 1$

equal to $\psi_{\text{th}} = 10^{-10}$. Owing to the stochastic behaviour of the PSO, 50 different simulations have been executed by randomly changing the initial particle swarm. Fig. 3*a* shows the pulse sequence $\boldsymbol{\tau}^{\text{rec}}$ providing the minimum value of the cost function (6) among the different runs, whereas the corresponding power pattern is given in Fig. 3*b*. As it can be noted (Fig. 3*b*), the pattern radiated by the reconfigured sequence has a SLL very close to the nominal one $\left(\text{SLL}^{\text{rec}}_{\text{Case A}} = -29.96\ \text{dB}\right)$, only 0.04 dB above the target value SLL^{nom}. As expected, the arising values of the other

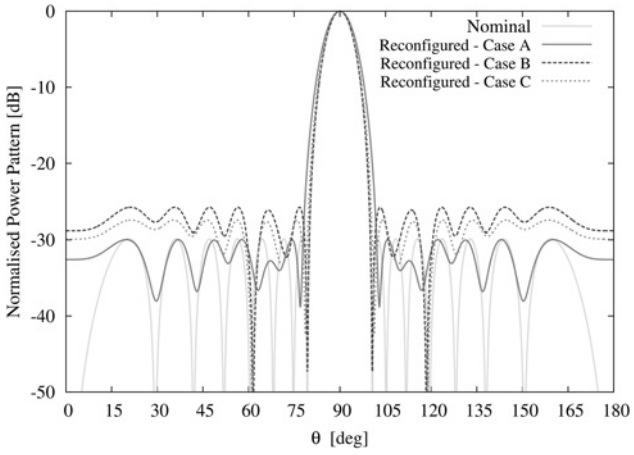

Fig. 6 *Case A, B and C – [N = 16, d = (λ/2), Dolph–Chebyshev, SLL = −30 dB, ϒ = {2}] – plots of the power pattern generated at f_0 together with the nominal one when $w_{SLL} = 1$ and $w_{HPBW} = w_D = 0$ (Case A), $w_{SLL} = w_{HPBW} = w_D = 1$ (Case B) and $w_{SLL} = 10$ and $w_{HPBW} = w_D = 1$ (Case C)*

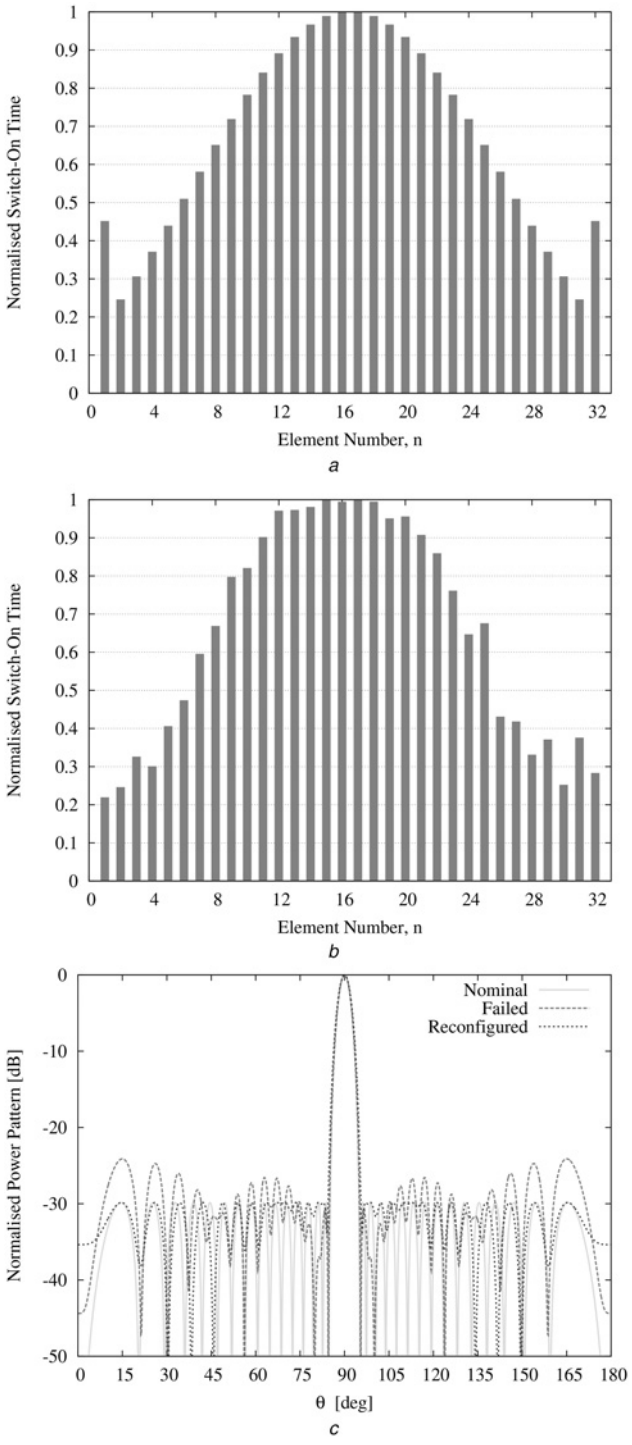

Fig. 7 *Case D – [N = 32, d = (λ/2), Dolph–Chebyshev, SLL = – 30 dB, ϒ = {2, 29}] – plots of*

a Nominal pulse sequence $\boldsymbol{\tau}^{\text{nom}}$

b Reconfigured pulse sequence $\boldsymbol{\tau}^{\text{rec}}$

c Reconfigured, nominal and failed power patterns generated at f_0 when $w_{\text{SLL}} = 10$ and $w_{\text{HPBW}} = w_D = 1$

doi: 10.1049/iet-rsn.2013.0027

pattern features ($\mathrm{HPBW}^{\mathrm{rec}}_{\mathrm{Case\ A}} = 9.16^{\circ}$ and $D^{\mathrm{rec}}_{\mathrm{Case\ A}} = 9.73$ dB) are worse with respect to the nominal indices as well as those of the failed arrangement (Table 1 – 'reconfigured': Case A) since neither the bandwidth nor the directivity have been taken into account in the optimisation, being $w_{\mathrm{HPBW}} = w_D = 0$.

When also considering the matching with $\mathrm{HPBW}^{\mathrm{nom}}$ and D^{nom} (i.e. $w_{\mathrm{SLL}} = w_{\mathrm{HPBW}} = w_D = 1$ – Case B), the PSO-optimised pulse sequence (Fig. 4*a*) synthesises the power pattern in Fig. 4*b*. Unlike Case A, the values $\mathrm{HPBW}^{\mathrm{rec}}_{\mathrm{Case\ B}}$ and $D^{\mathrm{rec}}_{\mathrm{Case\ B}}$ are closer to the reference ones

$$\Delta^{\mathrm{HPBW,\ rec}}_{\mathrm{Case\ B}} = \frac{\left|\mathrm{HPBW}^{\mathrm{rec}}_{\mathrm{Case\ B}} - \mathrm{HPBW}^{\mathrm{nom}}\right|}{\left|\mathrm{HPBW}^{\mathrm{nom}}\right|} = 1.6 \times 10^{-2} \text{ against } \Delta^{\mathrm{HPBW,\ rec}}_{\mathrm{Case\ A}} = 1.5 \times 10^{-1}$$

Table 2 Cases D and E – [$N = 32$, $d = (\lambda/2)$, Dolph–Chebyshev, SLL = –30 dB] – values of the pattern features SLL, HPBW and D and of the SBL and the percentage of SR losses with respect to the total radiated power for the nominal, failed and reconfigured solution when $\Upsilon = \{2, 29\}$ (Case D) and $\Upsilon = \{18\}$ (Case E)

	SLL, dB	HPBW, degrees	D, dB	SBL, dB	SR, %
nominal	−30.00	3.88	13.29	−12.29	23.95
Case D: $\Upsilon = \{2, 29\}$					
failed	−24.12	4.01	13.17	−12.77	22.58
reconfigured	−29.84	4.21	13.07	−13.54	23.66
Case E: $\Upsilon = \{18\}$					
failed	−19.34	3.91	12.94	−12.35	20.59
reconfigured	−23.87	4.02	12.67	−11.68	27.00

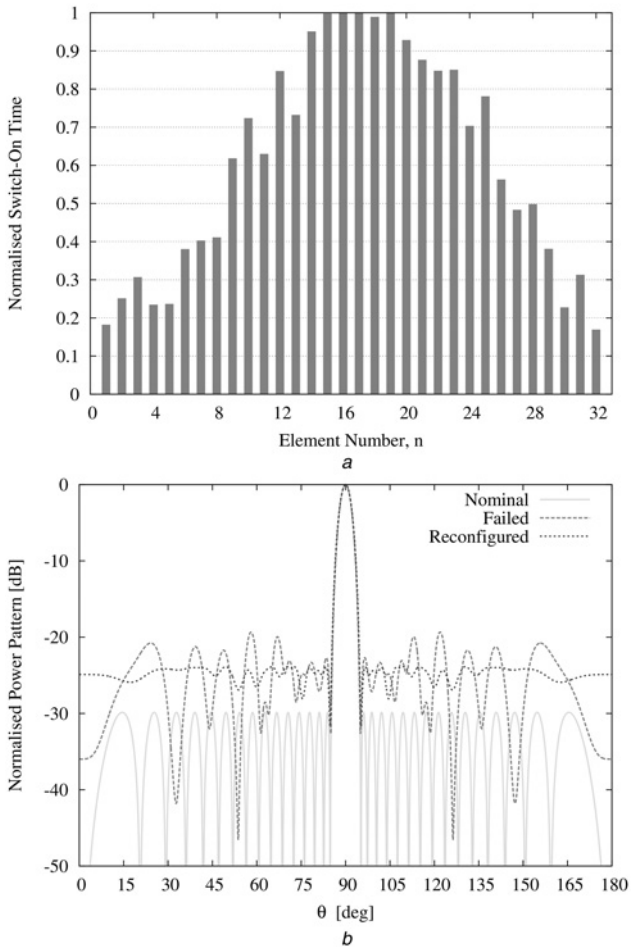

Fig. 8 *Case E – [N = 32, d = (λ/2), Dolph–Chebyshev, SLL = – 30 dB, Υ = {18}] – plots of*

a Reconfigured pulse sequence $\boldsymbol{\tau}^{\mathrm{rec}}$
b Corresponding power pattern generated at f_0 together with the nominal and failed ones when $w_{\mathrm{SLL}} = 10$ and $w_{\mathrm{HPBW}} = w_D = 1$

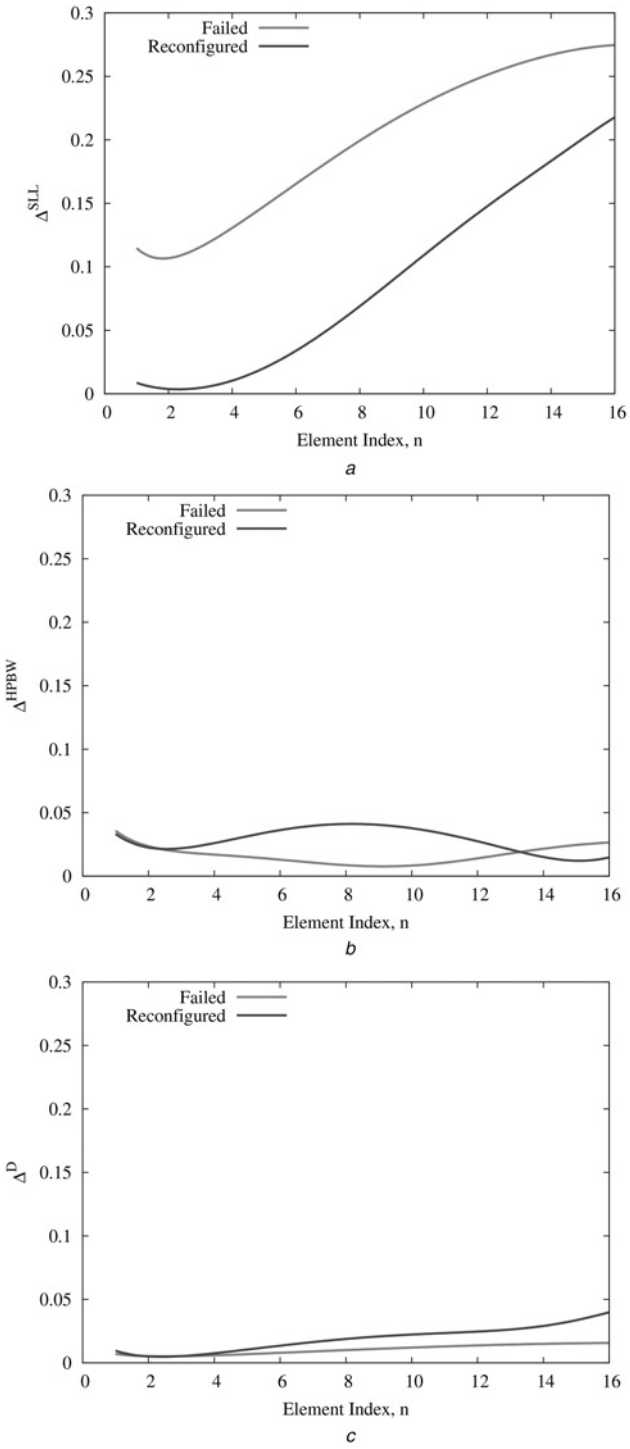

Fig. 9 *Case F – [N = 32, d = (λ/2), Dolph–Chebyshev, SLL = – 30 dB, Υ = {m}, m = 1, …, N] – behaviour of the parameter $\Delta^{fld/rec} = ((|\zeta^{fld/rec} - \zeta^{nom}|)/(|\zeta^{nom}|))$ for the failed and reconfigured solution when*

a $\zeta \Leftarrow$ SLL
b $\zeta \Leftarrow$ HPBW
c $\zeta \Leftarrow D$

Table 3 Case F – [$N = 32$, $d = (\lambda/2)$, Dolph–Chebyshev, SLL = −30 dB] – statistics (average, variance, minimum and maximum values) of the pattern features SLL, HPBW and D for the failed and reconfigured solution when $\Upsilon = \{m\}$, $m = 1,\ldots, N$

	SLL, dB		HPBW, degrees		D, dB	
	Failed	Reconfigured	Failed	Reconfigured	Failed	Reconfigured
avg	−23.94	−27.22	3.88	3.99	13.15	13.04
var	3.44	5.08	4.93×10^{-3}	2.42×10^{-3}	2.47×10^{-3}	1.88×10^{-2}
min	−27.11	−29.86	3.78	3.91	13.08	12.76
max	−21.66	−23.36	4.02	4.07	13.24	13.28

and

$$\Delta^{D,\,\mathrm{rec}}_{\mathrm{Case\ B}} = \frac{\left|D^{\mathrm{rec}}_{\mathrm{Case\ B}} - D^{\mathrm{nom}}\right|}{\left|D^{\mathrm{nom}}\right|} = 9.8 \times 10^{-4} \text{ against } \Delta^{D,\,\mathrm{rec}}_{\mathrm{Case\ A}} = 4.6 \times 10^{-2}$$

whereas the SLL turns out being higher ($\mathrm{SLL}^{\mathrm{rec}}_{\mathrm{Case\ B}} = -25.78$ dB against $\mathrm{SLL}^{\mathrm{rec}}_{\mathrm{Case\ A}} = -29.96$ dB).

The third case (Case C) is devoted to identify a weight condition where still giving priority (as in Case A) to keep the SLL close as much as possible to $\mathrm{SLL}^{\mathrm{nom}}$, HPBW and D are not heavily penalised. Accordingly, the following setup has been set: $w_{\mathrm{SLL}} = 10$ and $w_{\mathrm{HPBW}} = w_D = 1$. The reconfigured pulse sequence and the corresponding pattern are given in Figs. 5*a* and *b*, respectively. As expected, the features of the reconfigured pattern (Table 1) are a suitable compromise between the indices in Cases A and B as pictorially shown in Fig. 6 and confirmed by the indices in Table 1. In more detail, the values $\mathrm{HPBW}^{\mathrm{rec}}_{\mathrm{Case\ C}}$ and $D^{\mathrm{rec}}_{\mathrm{Case\ C}}$ are closer to the nominal ones as compared with the solution of Case A, but not considering the Case B, whereas $\mathrm{SLL}^{\mathrm{rec}}_{\mathrm{Case\ C}}$ improves with respect to the Case B, but it worsens with respect to the Case A. Although not directly considered in the optimisation step, the values of the sideband level (SBL), namely the peak level of the harmonics generated by the time-modulation process with respect to the peak of the array factor radiated at the carrier frequency f_0 [29], and of the amount of power losses in the sideband radiation (SR) [30] are reported in Table 1 for the sake of completeness. As can be observed, the reconfigured arrays have similar (Case A) or even lower (Cases B and C) values of SBL and SR with respect to the nominal and failed ones, thus confirming the feasibility of the PSO-obtained solutions.

The second example deals with a wider array of $N = 32$ ($d = 0.5\lambda$). The nominal pulse sequence (Fig. 7*a*) has been set to generate a Dolph–Chebyshev sum pattern [28] with $\mathrm{SLL}^{\mathrm{nom}} = -30$ dB (Fig. 7*c*). Two failures have been supposed to be present at the TMLA elements $m = 2$ and $m = 29$ (i.e. $\Upsilon = \{2, 29\}$). By considering $S = N = 32$ particles of the swarm and setting $w_{\mathrm{HPBW}} = w_D = 1$ and $w_{\mathrm{SLL}} = 10$, the best pulse configuration synthesised at the PSO convergence is that in Fig. 7*b* that affords the pattern given in Fig. 7*c*. The PSO optimisation turns out to be able to satisfy the condition $\mathrm{SLL}^{\mathrm{rec}}_{\mathrm{Case\ D}} \simeq \mathrm{SLL}^{\mathrm{nom}}$ ($\mathrm{SLL}^{\mathrm{rec}}_{\mathrm{Case\ D}} = -29.84$ dB against $\mathrm{SLL}^{\mathrm{nom}} = -30.00$ dB) with a non-negligible improvement with respect to the failed layout $\left(\mathrm{SLL}^{\mathrm{fld}}_{\mathrm{Case\ D}} = -24.12 \text{ dB}\right)$, whereas the matching of the remaining pattern features is less accurate (Table 2 – Case D) because of the unbalanced weighting.

Unlike the previous case where both failures were located in the tails of the array, let us suppose now having just one failure at the central element $m = 18$ (i.e. $\Upsilon = \{18\}$) (Case E). Of course, the effect on the pattern features is more evident and destructive as confirmed by the values of the pattern descriptors in Table 2. As a matter of fact, $\Delta^{\mathrm{SLL,\,fld}}_{\mathrm{Case\ E}} = 3.6 \times 10^{-1}$ is greater than $\Delta^{\mathrm{SLL,\,fld}}_{\mathrm{Case\ D}} = 2.0 \times 10^{-1}$ as well as $\Delta^{D,\,\mathrm{fld}}_{\mathrm{Case\ E}} = 2.6 \times 10^{-2}$ compared with $\Delta^{D,\,\mathrm{fld}}_{\mathrm{Case\ D}} = 9.0 \times 10^{-3}$. Differently, HPBW is only slightly perturbed ($\Delta^{\mathrm{HPBW,\,fld}}_{\mathrm{Case\ E}} = 7.7 \times 10^{-3}$ against $\Delta^{\mathrm{HPBW,\,fld}}_{\mathrm{Case\ D}} = 3.4 \times 10^{-2}$). After the optimisation ($w_{\mathrm{HPBW}} = w_D = 1$ and $w_{\mathrm{SLL}} = 10$), the synthesised time sequence (Fig 8*a*) generates a peak level of the secondary lobes equal to $\mathrm{SLL}^{\mathrm{rec}}_{\mathrm{Case\ E}} = -23.87$ dB, much above the desired one (Fig. 8*b* – Table 2). The values of SBL and SR for Cases D and E are reported in Table 2 as well.

As expected, the analysis points out that not only the number of failures, but also the position of the failed elements within the array aperture has an impact on the correction capability of the TMLA architecture, besides on the corruption of the nominal pattern. To further assess the effect of the failure positions on the pattern features, the index of the failed element has been varied within the range $m \in [1;\ 16]$ and only half array positions have been considered because of the symmetry of the nominal pulse sequence (Fig. 7*a*). Still setting $w_{\mathrm{HPBW}} = w_D = 1$ and $w_{\mathrm{SLL}} = 10$, the behaviours of $\Delta^{\zeta,\mathrm{fld}}$ and $\Delta^{\zeta,\mathrm{rec}}$ ($\zeta = \{\mathrm{SLL}, \mathrm{HPBW}, D\}$) against the failure location are reported in Fig. 9. Likewise previous experiments, there is a trade-off between the $\mathrm{SLL}^{\mathrm{now}}$ matching and those of the other pattern features. Indeed, the plots of these latter in the reconfigured condition [i.e. HPBW (Fig. 9*b*) and D (Fig. 9*c*)] do not always outperform those of the failed configuration as in Fig. 9*a*. However, it must be pointed out that there is a difference of about one order in magnitude among the values in Fig. 9*a* and those in Figs. 9*b* and *c*. Moreover, the average improvement of the SLL over the failed configuration turns out to be of >3 dB (Table 3) and the values of $\mathrm{SLL}^{\mathrm{rec}}$ result very close to $\mathrm{SLL}^{\mathrm{nom}}$ in several cases (i.e. when $m \in [1;\ 4]$). For the sake of completeness, the statistics of the patterns features are reported in Table 3.

4 Conclusions

A technique for failure correction in TMLAs has been presented. The reconfiguration of the on–off behaviour of the undamaged array elements has been exploited to provide a countermeasure to the nominal pattern corruption because of the failures. The minimisation of a suitable cost function measuring the misfit between the values of the SLL, HPBW (HPBW) and peak directivity (D) of the nominal pattern and the reconfigured one has been carried out to update the original time sequences. The numerical results have shown that:

- The approach proves to be an effective tool for restoring the original pattern features especially when failures occur

doi: 10.1049/iet-rsn.2013.0027

at the array elements characterised by short on-times (i.e. small values of $\boldsymbol{\tau}^{\mathrm{nom}}$);

- A suitable selection of the cost function weights allows the designer to heavily constrain specific pattern features more critical for the application at hand;
- The efficiency in generating a reconfigured pattern close to the nominal one depends not only on the number of failures, but also on the failure position within the array.

5 References

1 Shanks, H.E., Bickmore, R.W.: 'Four-dimensional electromagnetic radiators', *Can. J. Phys.*, 1959, **37**, pp. 263–275

2 Kummer, W.H., Villeneuve, A.T., Fong, T.S., Terrio, F.G.: 'Ultra-low sidelobes from time-modulated arrays', *IEEE Trans. Antennas Propag.*, 1963, **11**, (6), pp. 633–639

3 Bickmore, R.W.: 'Time versus space in antenna theory', in Hansen, R.C. (Ed.): 'Microwave scanning antennas' (Academic, 1966), vol. III

4 Yang, S., Gan, Y.B., Qing, A.: 'Sideband suppression in time-modulated linear arrays by the differential evolution algorithm', *IEEE Antennas Wirel. Propag. Lett.*, 2002, **1**, pp. 173–175

5 Fondevila, J., Brégains, J.C., Ares, F., Moreno, E.: 'Optimizing uniformly excited linear arrays through time modulation', *IEEE Antennas Wirel. Propag. Lett.*, 2004, **3**, pp. 298–301

6 Yang, S., Gan, Y.B., Qing, A., Tan, P.K.: 'Design of a uniform amplitude time modulated linear array with optimized time sequences', *IEEE Trans. Antennas Propag.*, 2005, **53**, (7), pp. 2337–2339

7 Basak, A., Pal, S., Das, S., Abraham, A., Snasel, V.: 'A modified invasive weed optimization algorithm for time-modulated linear antenna array synthesis'. Proc. IEEE Congress on Evolutionary Computation, Barcelona, Spain, 18–23 July 2010, pp. 1–8

8 Poli, L., Rocca, P., Oliveri, G., Massa, A.: 'Harmonic beamforming in time-modulated linear arrays', *IEEE Trans. Antennas Propag.*, 2011, **59**, (7), pp. 2538–2545

9 Labate, M.G., Buonanno, A., D'Urso, M., *et al.*: 'Photoconductive switches for radar systems exploiting time domain'. Proc. Fifth European Conf. Antennas Propagation, Rome, Italy, 11–15 April 2011, pp. 2244–2245

10 Yang, S., Gan, Y.B., Tan, P.K.: 'A new technique for power-pattern synthesis in time-modulated linear arrays', *IEEE Antennas Wirel. Propag. Lett.*, 2003, **2**, pp. 285–287

11 Fondevila, J., Brégains, J.C., Ares, F., Moreno, E.: 'Application of time modulation in the synthesis of sum and difference patterns by using linear arrays', *Microw. Opt. Technol. Lett.*, 2006, **48**, (5), pp. 829–832

12 Tennant, A., Chambers, B.: 'Two-element time-modulated array with direction-finding properties', *IEEE Antennas Wirel. Propag. Lett.*, 2007, **6**, pp. 64–65

13 Chen, Y., Yang, S., Nie, Z.: 'Synthesis of optimal sum and difference patterns from time modulated hexagonal planar arrays', *Int. J. Infrared Millim. Waves*, 2008, **29**, (10), pp. 933–945

14 Aksoy, E., Afacan, E.: 'Thinned nonuniform amplitude time-modulated linear arrays', *IEEE Antennas Wirel. Propag. Lett.*, 2010, **9**, pp. 514–517

15 D'Urso, M., Iacono, A., Iodice, A.: 'Optimizing uniformly equally spaced and sparse excited time-modulated linear arrays'. Proc. 2011 IEEE Radar Conf., Kansas City, MO, USA, 23–27 May 2011, pp. 586–589

16 Wang, Y., Tennant, A.: 'Sidelobe control of a time-modulated reflector-array'. Proc. Loughborough Antennas Propagation Conf., Loughborough, UK, 12–13 November 2012, pp. 1–4

17 Zhu, Q., Yang, S., Zheng, L., Nie, Z.: 'A pattern synthesis approach in four-dimensional antenna arrays with practical element models', *J. Electromagn. Waves Appl.*, 2011, **25**, (16), pp. 2274–2286

18 Tong, Y., Tennant, A.: 'Sideband level suppression in time-modulated linear arrays using modified switching sequences and fixed bandwidth elements', *Electron. Lett.*, 2012, **48**, (1), pp. 10–11

19 Li, G., Yang, S., Chen, Y., Nie, Z.: 'A hybrid analog-digital adaptive beamforming in time-modulated linear arrays', *Electromagnetics*, 2010, **30**, (4), pp. 356–364

20 Chen, Y., Yang, S., Li, G., Nie, Z.: 'Adaptive nulling with time-modulated antenna arrays using a hybrid differential evolution strategy', *Electromagnetics*, 2010, **30**, (7), pp. 574–588

21 Poli, L., Rocca, P., Oliveri, G., Massa, A.: 'Adaptive nulling in time-modulated linear arrays with minimum power losses', *IET Microw. Antennas Propag.*, 2011, **5**, (2), pp. 157–166

22 Li, G., Yang, S., Chen, Y., Nie, Z.: 'A novel electronic beam steering technique time modulated antenna arrays', *Prog. Electromagn. Res.*, 2009, **97**, pp. 391–405

23 Tong, Y., Tennant, A.: 'Simultaneous control of sidelobe level and harmonic beam steering in time-modulated linear arrays', *Electron. Lett.*, 2010, **46**, (3), pp. 201–202

24 Rodriguez, J.A., Ares, F., Fernandez, M., Iglesias, R., Barro, S.: 'Rapid method for finding faulty elements in antenna arrays using far field pattern samples', *IEEE Trans. Antennas Propag.*, 2009, **57**, (6), pp. 1679–1683

25 Oliveri, G., Rocca, P., Massa, A.: 'Reliable diagnosis of large linear arrays – a Bayesian compressive sensing approach', *IEEE Trans. Antennas Propag.*, 2012, **60**, (10), pp. 4627–4636

26 Yang, S., Gan, Y.B., Qing, A., Tan, P.K.: 'Evaluation of directivity and gain for time-modulated linear antenna arrays', *Microw. Opt. Technol. Lett.*, 2004, **42**, (2), pp. 167–171

27 Rocca, P., Benedetti, M., Donelli, D., Franceschini, D., Massa, A.: 'Evolutionary optimization as applied to inverse scattering problems', *Inverse Probl.*, 2009, **25**, pp. 1–41

28 Elliott, R.S.: 'Antenna theory and design' (John Wiley & Sons, 2003)

29 Poli, L., Rocca, P., Manica, L., Massa, A.: 'Pattern synthesis in time-modulated linear arrays through pulse shifting', *IET Microw. Antennas Propag.*, 2010, **4**, (9), pp. 1157–1164

30 Poli, L., Rocca, P., Manica, L., Massa, A.: 'Handling sideband radiations in time-modulated arrays through particle swarm optimization', *IEEE Trans. Antennas Propag.*, 2010, **58**, (4), pp. 1408–1411